# FINITE ELEMENT WATER QUALITY MODELLING OF WWTP DISCHARGES AND RESUSPENDED SEDIMENTS IN THE BRISBANE RIVER ESTUARY AND MORETON BAY

**P Bell**[1] , J M$^{c}$Ewan[2]

[1]University of Queensland, St Lucia, QLD.
School of Chemical Engineering University of Queensland, Brisbane, Australia
PO Box 6214 St Lucia 4067
Tel: 0414170848 E-mail: p.bell@uq.edu.au
[2] M$^{c}$Ewan Consulting, Lismore, NSW.

## Abstract

2D and 3D versions of SHYFEM and RMA finite element computer models are used to assess the impacts of discharges from wastewater treatment plants (WWTPs), river inflows and the resuspension of sediments on the water quality in the Brisbane River estuary and Moreton Bay. The original codes have been extended to include additional water quality variables including 3 types of phytoplankton, namely, diatoms, dinoflagellates and N-fixing cyanobacteria. The SHYFEM model offers a particular advantage in 3D applications with computational speeds being an order of magnitude faster than those of the RMA model. However the RMA model can be operated in 1D mode in conjunction with 2D and 3D applications which is often useful in systems containing narrow channels. The results show that:

- the WWTP discharges have a significant impact on the dissolved oxygen and nutrient concentrations in the Brisbane-Bremer estuary;
- the nutrients discharged to Moreton Bay promote high levels of phytoplankton growth;
- floodwater discharges to Moreton Bay result in a significant amount of sediment being deposited in the Bay;
- the turbidity maximum in the Brisbane River estuary during “dry weather” results from the combined effects of tidal resuspension of the flocculating sediments and the density stratification induced by baseline freshwater flow;
- the turbidity in the Brisbane River estuary restricts phytoplankton growth; this turbidity could be reduced by restricting the tidal range and/or by reducing the baseline freshwater flow to the estuary.

## Introduction

Moreton Bay is located adjacent to the city of Brisbane on the east coast of Australia (Fig. 1) and is enclosed by barrier islands which are formed to a large extent by vegetated sand dunes. Water movement in the Bay and its estuaries is driven by mixed diurnal and semi-diurnal tides circulating through the northern entrance and to some extent through the southern passages, with tidal range of up to 2 m at Spring tides. Moreton Bay receives run-off via creeks and rivers from a number of catchments (see Fig. 1). Most dry-weather inflows occur through the four major estuaries: Brisbane-Bremer, Caboolture, Pine, and Logan-Albert. The Brisbane-Bremer River estuary extends some 90 km from the mouth, with salinity intrusion reaching 40 to 60 km upstream, depending on the amount of freshwater flow. The Brisbane River estuary is characterised by high turbidities with a maximum turbidity usually occurring near to the saline intrusion limit. Many domestic and industrial wastewater treatment plants (WWTPs) discharge to the estuaries and some others discharge directly to Moreton Bay. These point source discharges account for most of the external loads of nitrogen (N) and phosphorus (P) to the system and for a large proportion of the biodegradable carbon (i.e. BOD) (McEwan et al. 1998; McEwan, 1996; Bell et al. 2003). The models described herein were developed to investigate factors causing turbidity in the Brisbane-Bremer River estuary and the impacts of the WWTP discharges on Moreton Bay and its estuaries. The SHYFEM (Umgiesser et al. 2003; 2004) and RMA (King, 2005; 1997) finite element hydrodynamic and water quality models are applied in this work. The water quality relationships originally implemented in the programs were derived from WASP5 and QUAL2E (Ambrose et al., 1993; Brown and Barnwell, 1987).

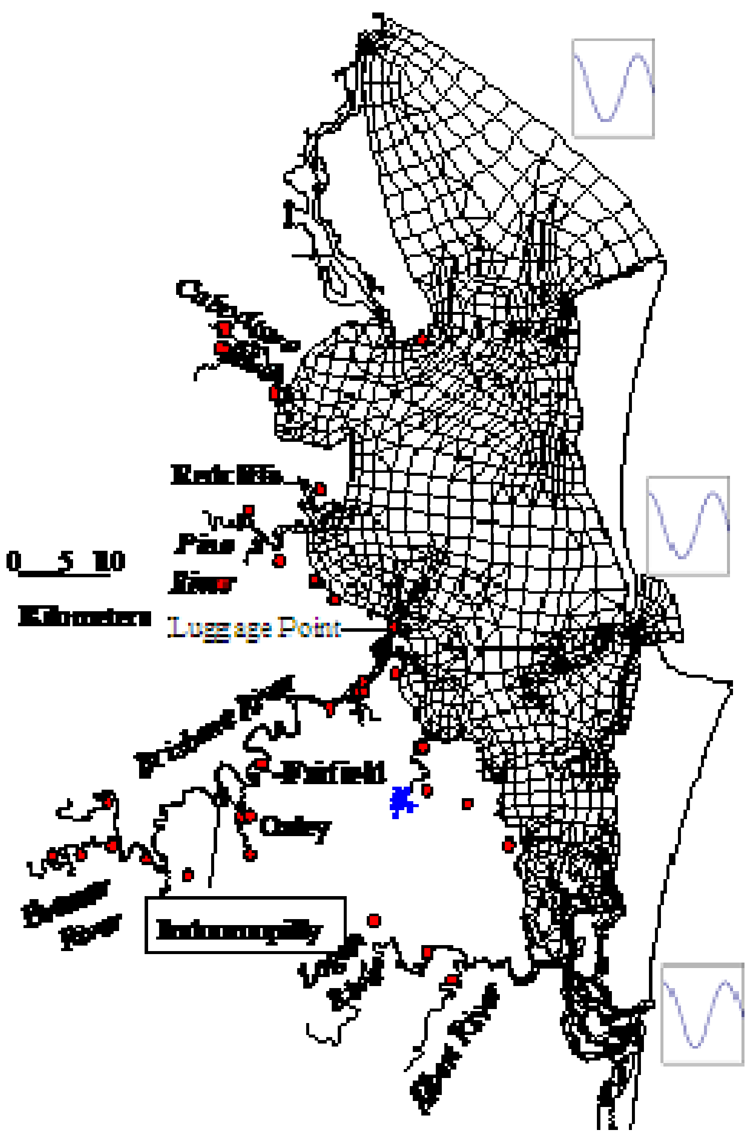


**Fig. 1: Moreton Bay-showing tidal boundaries, RMA finite element mesh, estuaries & WWTP locations (●) for year 2000**

The water quality codes can model various parameters in the water column and in the sediments associated with WWTP discharges and urban run-off (e.g. dissolved oxygen, $BOD_5$, bacteria, suspended sediment) as well as predict the resultant growth of algae due to the nutrient discharges. A simplified schematic of the principal factors affecting phytoplankton growth and the cycling/consumption of N, P and dissolved oxygen (DO) in the water column and sediments as considered by the models is shown in Fig. 2.

In addition to the N and P cycles depicted in Fig. 2 the finite element models have been extended to include the cycling of silicate (Si) and iron (Fe). Fe and Si are important chemical factors often controlling the competitive development of diatoms, dinoflagellates (e.g. red tide species) and N-fixing cyanobacteria (or blue-green algae) such as *Trichodesmium* spp. The models can also be used to study the growth of attached algae and drift algae (e.g. *Lyngbya* spp.). Further details of the processes considered in the water quality modules are given in Appendix A.

Four applications of the SHYFEM and RMA suite of programs are discussed below, namely applications of the: (i) 1D versions of RMA2 and RMA11 to the Brisbane-Bremer River estuary; (ii) 2D versions of RMA2 and RMA11 to the modelling of phytoplankton growth in Moreton Bay (iii) 3D versions of RMA10 and RMA11 to the modelling of turbidity in the Brisbane-Bremer River estuary (iv) 3D version of SHYFEM to modeling the impacts of flood-flows to Moreton Bay. All “dry-weather” model runs were carried out for average loads from the WWTPs for the year 2000. The year 2000 was a relatively dry year and hence the simulations are referred to as "dry-weather" simulations. “Flood-flow” simulations were done for the year 1996 for which significant inflows of floodwaters occurred between 30 April and 8 May (McEwan, 1998).

## Brisbane-Bremer River estuary model-1D RMA2 & RMA11

The model geometry used in this work includes the Brisbane-Bremer River estuary and associated tributaries. The tidal elevations at the lower Bay boundary were derived from the full Moreton Bay model. Flows at the upper boundaries were estimated from available gauged data. The RMA11 model set-up was a simplified version of that depicted in Fig. 2. In particular phytoplankton growth was not considered and interactions between the water column and the sediments were ignored (Bell et al., 2003). Also the model was set up as a 1D model i.e. water quality constituents were treated as varying along the length of the estuary but not in vertical or lateral directions. These simplifications were based on information gained from various sampling programs e.g. the Queensland Environmental Protection Agency (QEPA) field data shows that little or no phytoplankton growth occurs over most of estuary; this being attributed to the relatively high turbidity that results from the high concentrations of cohesive suspended solids (CSS or SS). These data also show that there is little or no exchange of filterable reactive phosphorus (FRP or $OPO_4$) with the CSS and other data collected by CSIRO shows that there was little exchange of P with the bed.

Thus this simplified model investigates the following water quality constituents: dissolved oxygen (DO), ammonium nitrogen (NH4), oxidised nitrogen (NOx), organic nitrogen (ON); inorganic phosphorus (FRP) and organic phosphorous (OP) and organic carbon (CBOD), both labile and semi-labile components are considered. Salinity variations were used to calibrate the transport processes in the lower Brisbane River estuary for this "dry weather” situation and FRP was used to calibrate the transport processes in the upper Brisbane-Bremer River.

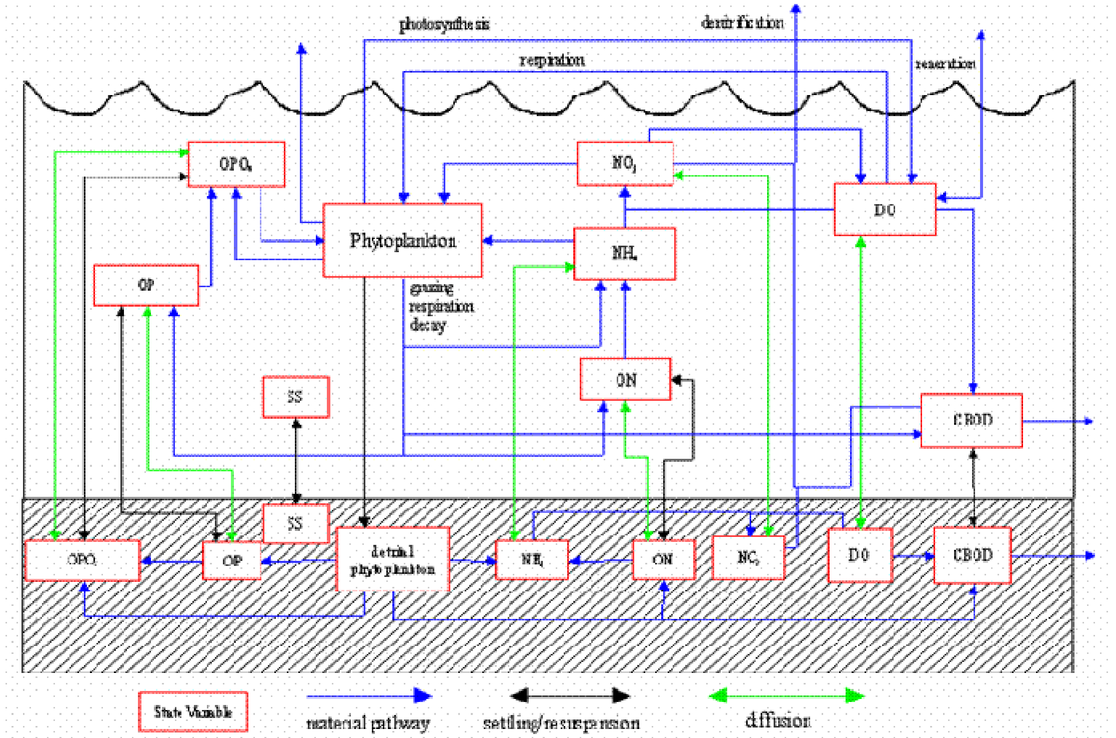


**Fig. 2. Schematic showing principal model pathways of nitrogen, phosphorus, CBOD and dissolved oxygen in the water column and sediments**.

Calibration of the transport model requires specification of the longitudinal dispersion coefficient. As noted above salinity distributions were used to calibrate the dispersion characteristics of the model in the lower reaches of the Brisbane River estuary and FRP distributions were used in the upper estuarine reaches and in Moreton Bay. The dispersion coefficient, $D_L$ ($m^2/s$), was assumed to be of the following form:

$$D_L = A^* \, U \, H \qquad (1)$$

where:

A* is a dimensionless calibration parameter
U is the instantaneous magnitude of the depth-averaged velocity (m/s)
H is the depth of the section (m)

Equation (1) has some theoretical foundation; previous work has shown that A* would increase with the width:depth ratio (W/H) and with the Manning's friction coefficient (n) (Bell et al. 2003). The calibration showed that A* reduced in magnitude from 90 at the mouth to 20 in the upper reaches of the Brisbane River below the junction with the Bremer River. In the vicinity of the Brisbane-Bremer junction W/H is much greater than that in the Brisbane River below the junction. A* was set to 55 in this region.

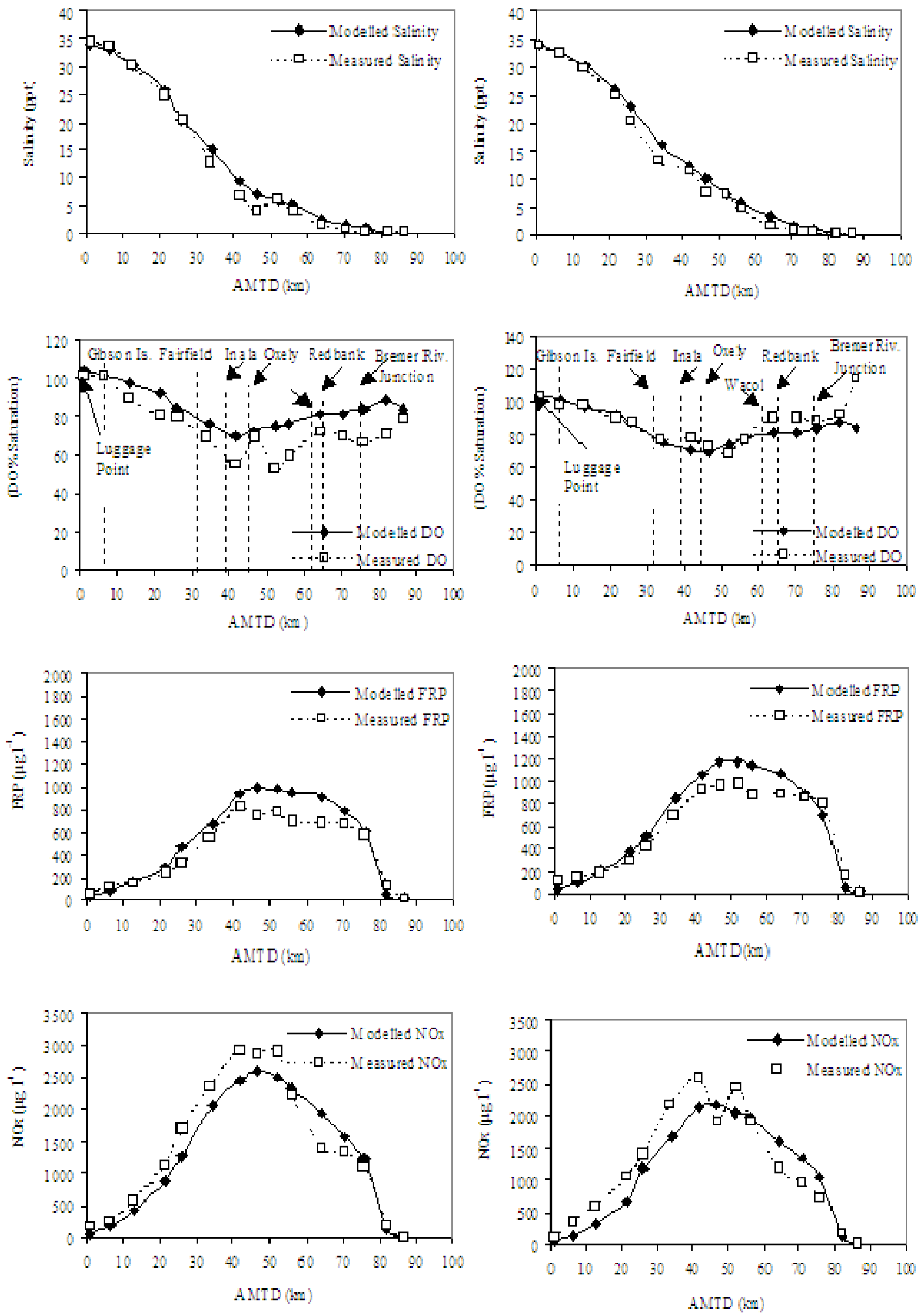


**Fig. 3: Comparison of modelled and measured (QEPA) water quality parameters along the Brisbane River estuary for Survey 3 and Survey 5.**

In the shallow sections of the Bremer River above the junction, W/H is relatively high and the Manning's coefficient is also relatively high. Hence a relatively high value of A* i.e. 35 was chosen for these sections. Fig. 3 shows a comparison between the measured and computed salinity and FRP distributions for 2 out of the 8 surveys during the year 2000. Overall the predictions for all 8 surveys were in excellent agreement with the recorded time series of salinity and FRP data.

### *Water quality predictions in Brisbane River estuary*

Model predictions were carried out for the mean loads from the various WWTP discharges for the year 2000*.* The results show that the predicted distributions of nutrients and dissolved oxygen are in excellent agreement with the time series of field data (Fig. 3). The results demonstrate the recorded oxygen sag can be directly attributed to the WWTP discharges. Also the results demonstrate that the WWTP loads alone are responsible for the high concentrations of nutrients in the Brisbane-Bremer River estuary during dry-weather. It is noted that FRP adsorption by the CSS (and sediments) and denitrification were set to zero in these simulations yet there is excellent agreement between the measured and modeled distributions. These results suggest that denitrification in the estuary was minimal and provide further evidence that FRP adsorption by the CSS (and sediments) was minimal.

## Prediction of turbidity in Brisbane-Bremer estuary-3D RMA10 & RMA11

Prediction of turbidity in the Brisbane-Bremer estuary requires application of the 3D versions of RMA10 and RMA11 because the transport of cohesive sediment is largely driven by vertical flow asymmetry which in turn is driven by density stratification effects of salinity (Bell et al., 2002; 2003). Fig. 4 shows the predicted vertical and longitudinal variations in salinity (from RMA 10) for normal "dry-weather" flow conditions in the Brisbane River estuary during the ebb and flood tides. These results suggest that significant stratification occurs during the ebb tide while little or no stratification occurs during the flood tide. RMA 11 uses the predicted salinity distributions and velocity fields from RMA 10 to solve the transport equations for the CSS. There are 4 principal factors that control the vertical movement of sediment from the bed surface:

- Applied shear stress $\tau_a$ : total shear stress due to tidal and wind effects, calculated dynamically for each model element.
- Critical deposition shear stress $\tau_d$ : a global input value.
- Critical erosion shear stress $\tau_e$ : a global input value, one for each layer.
- Effective settling velocity of sediment.

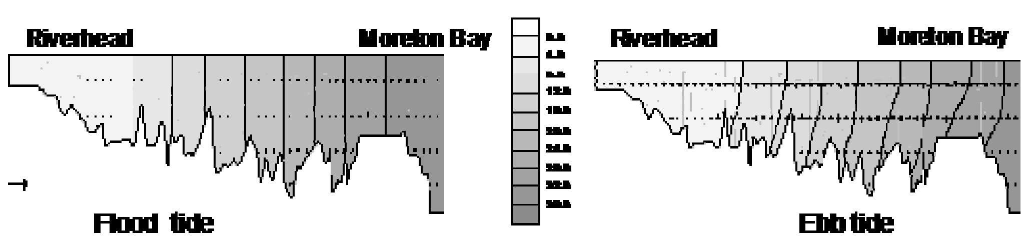


**Fig. 4: Predicted vertical and longitudinal salinity variations along the Brisbane River.**

The quantitative relationship between the shear stress parameters defines 3 settling regimes (Bell et al. 2003; McEwan, 1998):

*1:* $\tau_a < \tau_d$ *: applied shear below the critical deposition shear*
Sediment settles to the bed. The effective settling rate increases to a maximum as applied shear stress tends towards zero to represent the increased probability of deposition. There is no erosion during this regime.
*2:* $\tau_d < \tau_a < \tau_e$
Sediment remains in suspension and is advected by the local velocity field until it is either flushed out of the system across the downstream boundaries or reaches a zone where local shears are low enough for it to settle to the bed. There is neither erosion nor deposition during this regime.
*3.* $\tau_e < \tau_a$ *: applied shear above the critical erosion shear*
Sediment erodes from the bed. All layers above the bottom layer are considered unconsolidated and erode *en masse*, while the bottom layer erodes gradually at a rate proportional to the excess shear stress.

### *Turbidity model set-up*

A tidal boundary was applied at the Moreton Bay end of the Brisbane River; the elevations were obtained from an RMA2 simulation for the full Bay model. The salinity at the Moreton Bay boundary was set to a constant value of 34.5ppt on the incoming tide; this is a typical "dry-weather" value. Upstream boundary flows were gauged flows corrected for known off-takes. Up-stream inflow salinity concentrations were set to a nominal 0.1ppt. Constant element inflows were used to represent the discharges from the WWTPs. The boundary value for cohesive suspended solids (CSS) at the Moreton Bay end of the Brisbane River was set to a nominal 10 mg $l^{-1}$. This is a typical mean value for the western side of Moreton Bay near to the river mouth. Few data are available for sediment inputs at the upper boundary so nominal values were used, namely 0 mg $l^{-1}$ during low flows (<$3m^3s^{-1}$) and 200 mg $l^{-1}$ during high flows (> $3m^3s^{-1}$).

### *Calibration and Validation of turbidity model*

Data from the QEPA continuous recording turbidity meter at Indooroopilly was used to calibrate and validate the model. This turbidity data is recorded as NTU but the model predicts the concentration of CSS (mg $l^{-1}$) in the water column. In order to compare the model output with the measured turbidities a correlation between CSS (mg $l^{-1}$) and turbidity (NTU) is required. A comparison of the available data (Bell et al. 2002) suggests the following simple correlation is a reasonable estimate for the region under study:

$$\text{CSS (mg } l^{-1}) = 1.0 * \text{NTU} \qquad (2)$$

The model was calibrated over a Spring-Neap tidal cycle during January 2001 and verified to against the December 2000 data (Fig. 5). The number of adjustable parameters was minimised by using values determined by field measurements. In particular measured values for the critical erosion and deposition shear stresses, and the erosion rate were used (Bell et al. 2002). The principal "tuning" parameters are the settling velocity parameter $V_s$ and the particulate vertical diffusion coefficient $D_z$. A value of $V_s$ equal to 8 m $hr^{-1}$ was required to match the minimum CSS concentration at slack water. The experimental results show a rapid rise in turbidity on both a rising and falling tide. A relatively high particle dispersion parameter ($D_z$=0.5 $m^2$ $s^{-1}$) was chosen to overcome the high settling rate and thus mimic this rapid rise in turbidity. At first glance the values used for $D_z$ and $V_s$ look high but it needs to be recognised that these parameters are not simply the settling rate and vertical diffusion rate of a single particle size. These parameters have to encapsulate many complex dynamic mechanisms such as agglomeration, flocculation and floc breaking.

### *Turbidity time-series at Indooroopilly*

Fig. 5 shows a comparison of the variations in the predicted and measured turbidity over a Spring-Neap tidal cycle. Overall there is very good agreement between the measured and predicted time series. The results show that peak “dry-weather” turbidities occur during the Spring tide periods and that turbidity maxima occur on both the flood and ebb tides. These peaks result from resuspension events that occur when the bottom shear stress exceeds the critical shear stress. Also the highest turbidities generally occur on the flood tide. The reason for this is twofold. Firstly the velocity magnitude at depth (and hence bed-shear) on the flood tide is generally greater than that on the ebb tide. Secondly vertical mixing of the turbidity is restricted more during the ebb tide due to the effects salinity stratification ( see Fig. 4).

As noted above the results from the continuous turbidity recorder at Indooroopilly and the modelled results (see Fig. 5) show that the highest turbidities in “dry-weather” occur during the Spring tide period. These results suggest that if the tidal range could be reduced to the normal neap range (e.g. by building a partial tidal barrier) then dry-weather maximum turbidity would be reduced to around 50 NTU compared with the present 150-200 NTU.

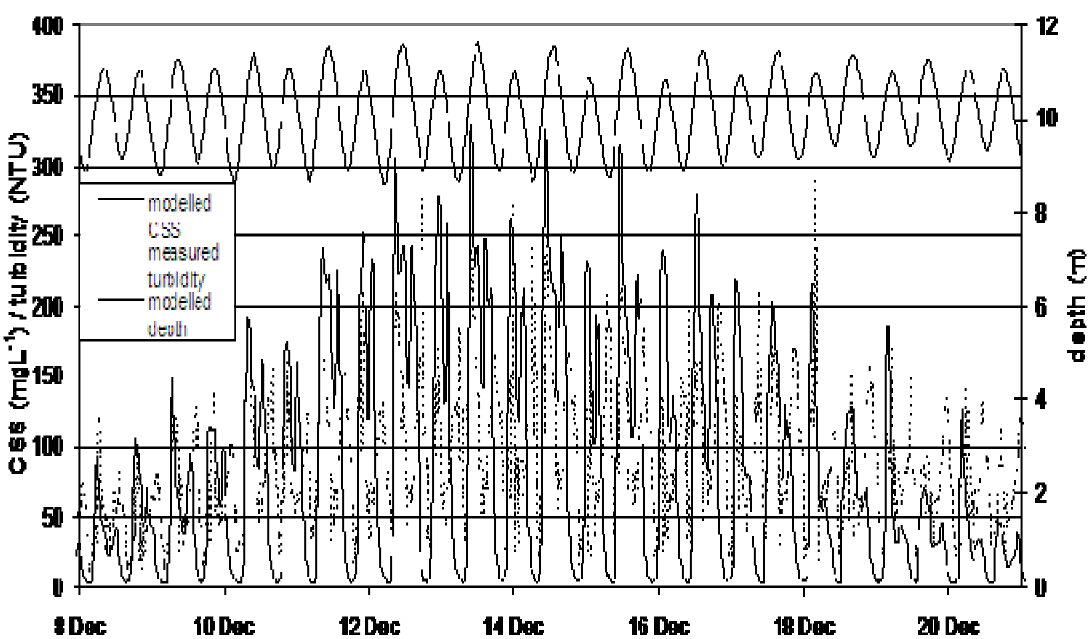


**Fig.5: Comparison of measured (QEPA) and predicted turbidity at over a Spring-Neap cycle**

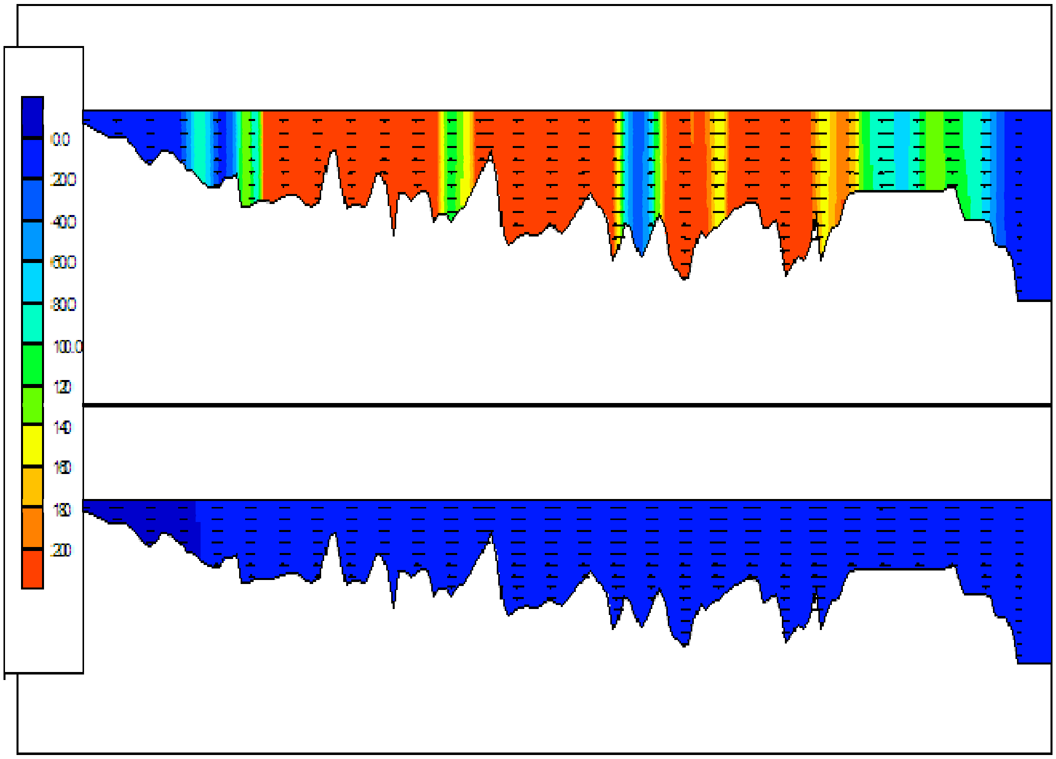

**Fig 6. Predicted effect of a reduction in freshwater inflows. on “dry-weather” turbidity (NTU) distribution in Brisbane River**

### *Effect of Moreton Bay turbidity on Brisbane River turbidity*

A six-month model run was conducted to examine the importance of Moreton Bay as a source of turbidity in the Brisbane River. The run conditions were as follows: initial turbidity throughout the estuary was set to zero; initial sediment thickness throughout the estuary was set to zero; turbidity at the Moreton Bay boundary was set to 20 NTU (i.e. CSS = 20 mg/l) on the flood (incoming) tide; freshwater inflow as per gauged-flows (with CSS = 0.0) as determined for January to June year 2000. The results show (Fig. 7) that the maximum turbidity at Indooroopilly increases with time and that after 6 months is at levels several times that at the boundary and in fact is similar to the “normal” dry-weather” turbidity (see Fig. 5)

### *Effect of reducing freshwater base-flow and tidal range on turbidity*

The effect of reducing the upstream freshwater flow to zero was examined by repeating the above analysis i.e. examining the case for which the only source of CSS is Moreton Bay but in this case reducing the upstream freshwater inflows to zero. A comparison of the results for this case (Fig.6 and Fig. 8) with those for the case of normal freshwater flow (Fig 6 and Fig. 7) shows that reducing the freshwater flow causes a dramatic reduction on the predicted turbidity. The reason for this is that, with no freshwater flow, the upstream pumping mechanisms brought about by stratification within the estuary are eliminated. The minimal amount of turbidity that is transported upstream during the “no freshwater flow” situation results from dispersion and dynamic settling/resuspension phenomena.

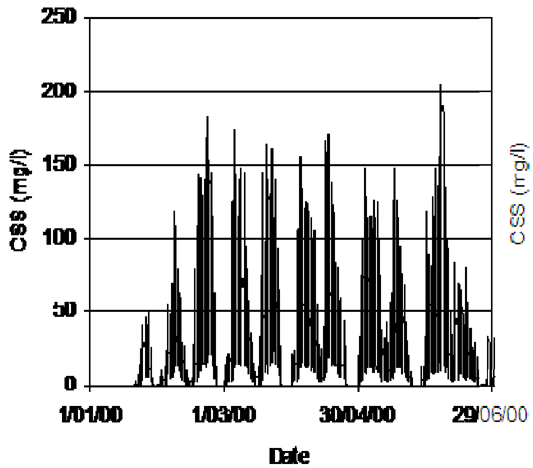


Fig.7: **Predicted turbidity at Indooroopilly for normal freshwater flow and CSS sourced only from Moreton Bay.**

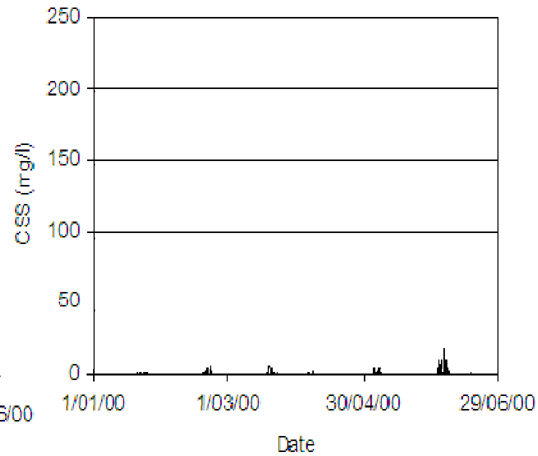


**Fig.8: Predicted turbidity at Indooroopilly for no freshwater flow and CSS sourced from Moreton Bay**.

## Modelling Water Quality in Moreton Bay-2D RMA2 & RMA11

RMA2 was used to model the 2D hydrodynamics of Moreton Bay with applied year 2000 tidal boundary conditions and winds. Lateral and longitudinal dispersion coefficientients in Moreton Bay were assumed to be governed by equation (1). As noted above, salinity was used for determining A* in the lower reaches of the Brisbane River estuary but due to small variations in salinity throughout the Bay during "dry-weather" and the low precision of the methods used for the measurement of salinity it was decided to investigate the usefulness of using FRP as a passive tracer in Moreton Bay. The reasons we chose FRP are:

- the phytoplankton growth within the Bay is generally considered to be saturated with respect to phosphorus (McEwan et al. 1998; McEwan, 1996; Bell et al. 2003);
- the principal "dry-weather" source of FRP is WWTP effluent and the concentration of FRP in the WWTPs is relatively high (average flow-weighted concentration of FRP is 6 mg/l i.e. 6000 µg/l) in comparison with background oceanic values (~2 µg/l);
- FRP is readily measured down to very low concentrations (detection limit ~1µg/l);
- FRP does not appear to react with or adsorb readily to the particulates in the estuaries (Bell et al 2003)

A* was determined (best fit obtained with A*=90) using the 1993 data set of McEwan (1996) (Bell et al. 2003). The RMA11 transport model was validated by comparing the predicted contour plots for FRP with those obtained from the QEPA 2000 field data (see Fig. 9). The results show excellent agreement between the measured and predicted FRP results throughout the Bay.

Analysis of the field data for Moreton Bay shows that there is a strong correlation between mean (time averaged) FRP and mean chlorophyll *a* (Fig. 10) and hence we investigated the possibility of using the FRP results to predict the distribution of chlorophyll *a*. The results of this prediction (Fig. 11) are in excellent agreement with the measured values of chlorophyll *a*. We suggest the good correlation between FRP and chlorophyll *a* results from the fact that FRP is present far in excess of that required for phytoplankton growth throughout most of the Bay and hence the correlation between FRP and chlorophyll *a* can be interpreted as a correlation between the availability of limiting nutrients (e.g. N), as supplied from WWTP discharges (and hence effluent dilution), and phytoplankton growth.

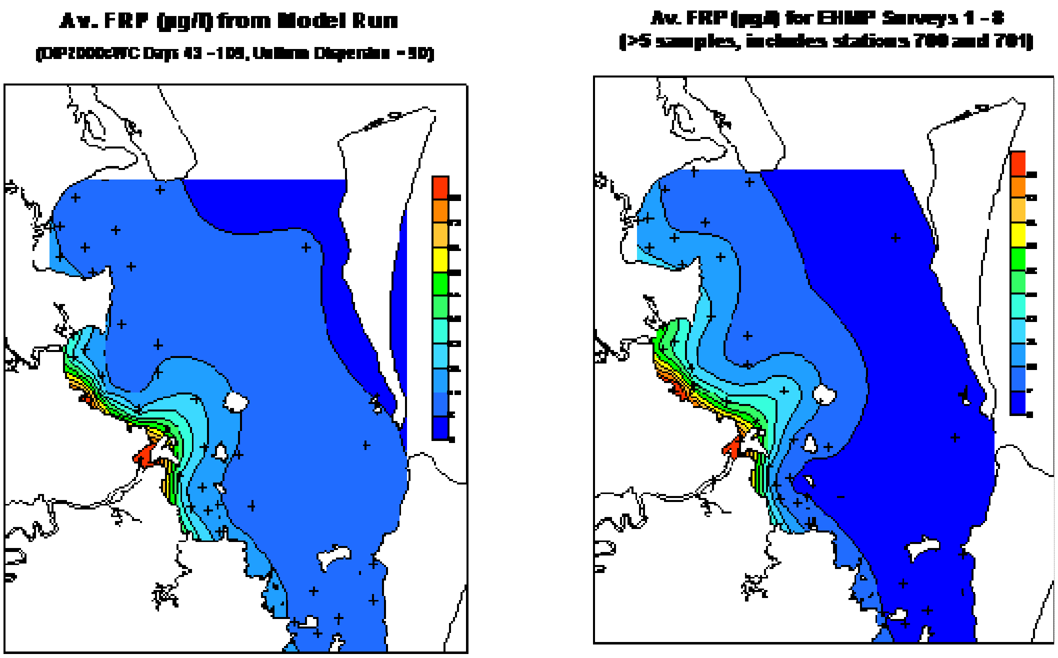


**Fig. 9 Comparison of the predicted contour plots for FRP with those obtained from the QEPA 2000 field data**

This correlative approach allows for exploration of scenarios such as the effects of reduction in particular WWTP discharges on the distribution of chlorophyll *a* in Moreton Bay by simply treating FRP as a passive tracer and then modeling the distribution of FRP. The predicted FRP distributions can then be used with the correlation in Fig. 10 to predict the chlorophyll *a* distribution e.g. Fig. 12 shows the predicted effects of removal of the Luggage Point WWTP discharge on the chlorophyll *a* distribution. In Fig. 12 the region of chlorophyll *a* >1 µg/l corresponds to FRP >12 µg/l as per data in Fig.10.

### *Preliminary calibration of full phytoplankton growth model for Moreton Bay*

Full calibration of the RMA11 model depicted in Fig. 2 for the prediction of phytoplankton growth in the Bay is a very complex task, it requiring the specification of many model parameters. This is an on-going task and hence only preliminary results will be presented here. Initial choice of the model parameters was based on those used by McEwan (1996). Fig. 13 shows the predicted output of the chlorophyll *a* distribution for the mid-tide situation during April 2000. These preliminary results are in general agreement with the field data given in Fig. 11.

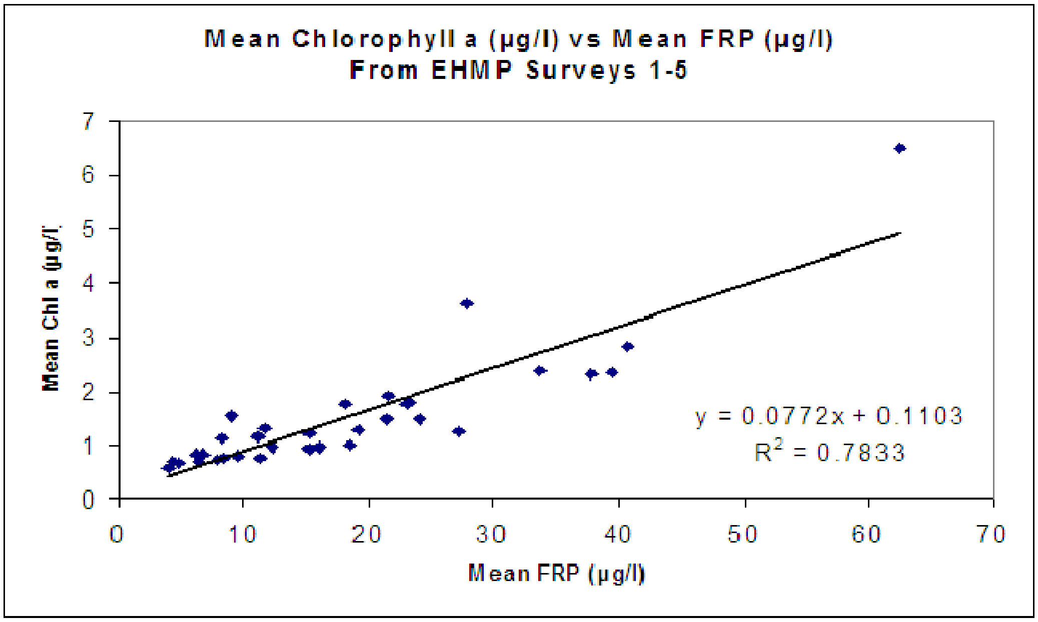


**Fig. 10. Correlation between Mean FRP and Mean Chlorophyll *a* for all stations year 2000.**

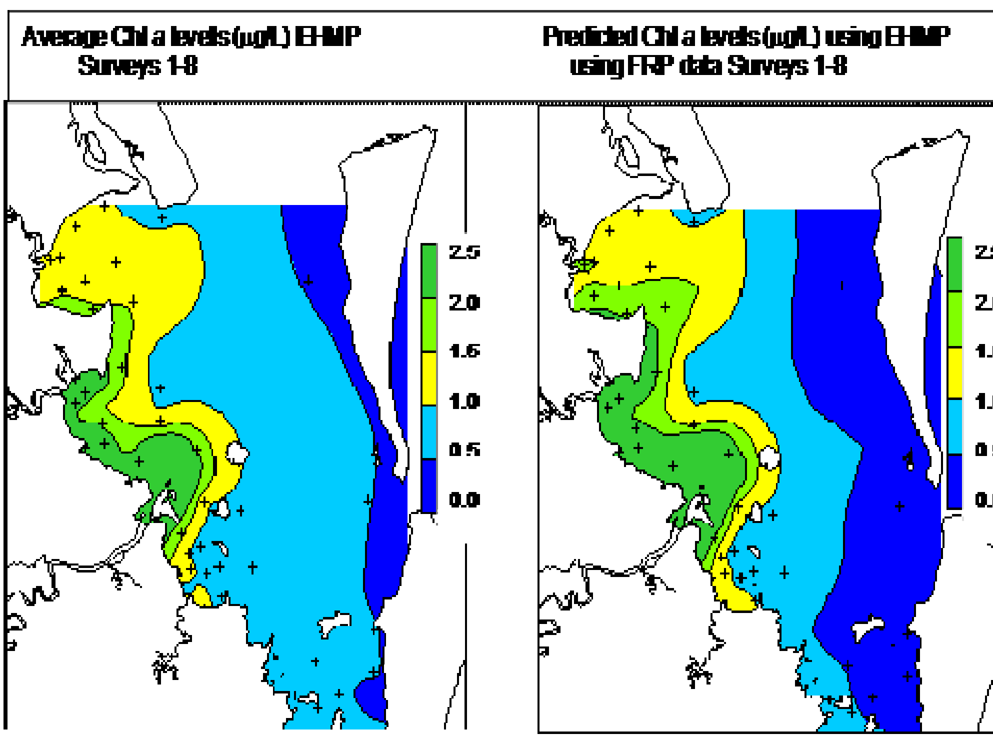


2.5
2.0
1.5
1.0
0.5
0.0

**Fig. 11. Comparison of predicted and measured mean chlorophyll *a* distributions in Moreton Bay using a simplified correlative prediction based on the distribution of FRP**

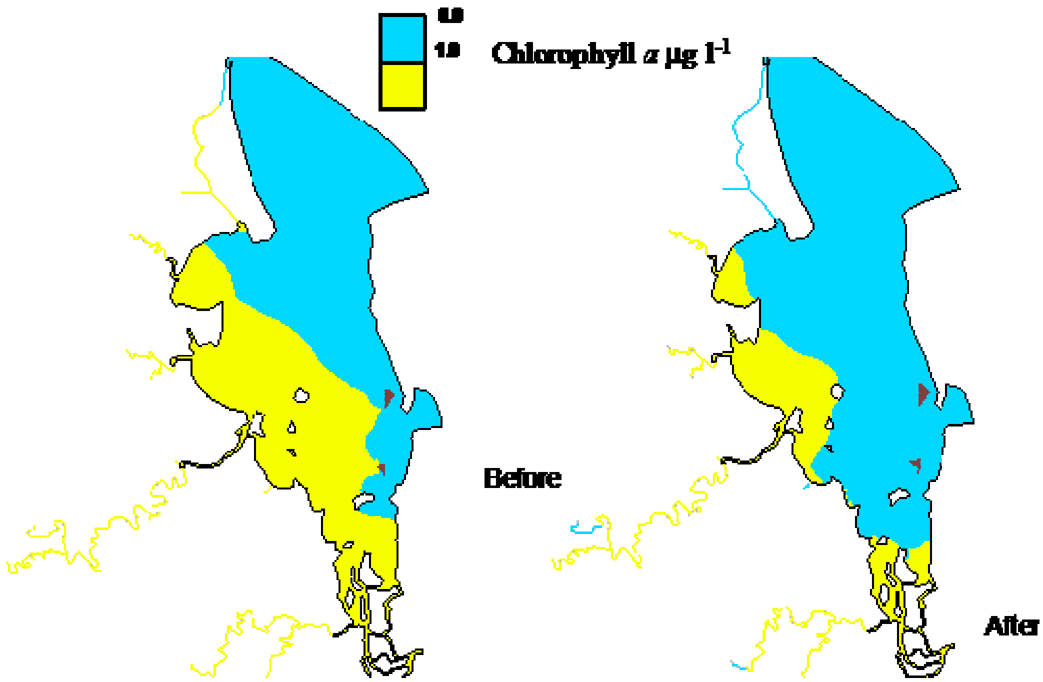


**Fig. 12: Predicted distributions of chlorophyll *a* before and after removal of Luggage Point WWTP discharge using a correlative model.**

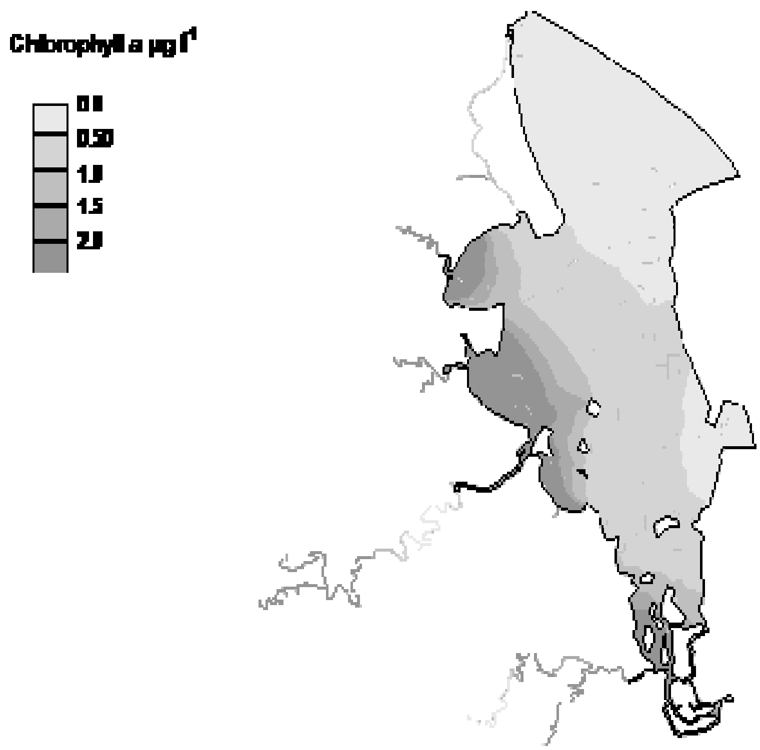


**Fig. 13: Predicted distribution of chlorophyll a using full 2D RMA11 nutrient/eutrophication model depicted in Fig. 2**

***Evaluation of the impacts of discharges from Luggage Point and Gibson Island WWTPs on the distribution of fecal coliforms***

The impacts of the discharges from Luggage point and Gibson Is. WWTPs on fecal coliform concentrations in the waterways was evaluated. A concentration of 400,000 coliforms per litre is assumed in each discharge. A constant temperature of 22$^o$C is assumed and the turbidity is assumed constant (equivalent to a $K_d$ of 0.7). A contour plot of the predicted distribution of fecal coliforms is shown in Fig. 14. The longitudinal distribution of fecal coliforms in the lower Brisbane River is compared with the available field data from QEPA in Figure 14.

The predicted and measured results suggest that the impact of these fecal coliform discharges is restricted to the lower reaches of the Brisbane River (0-20 km) and nearby Moreton Bay.

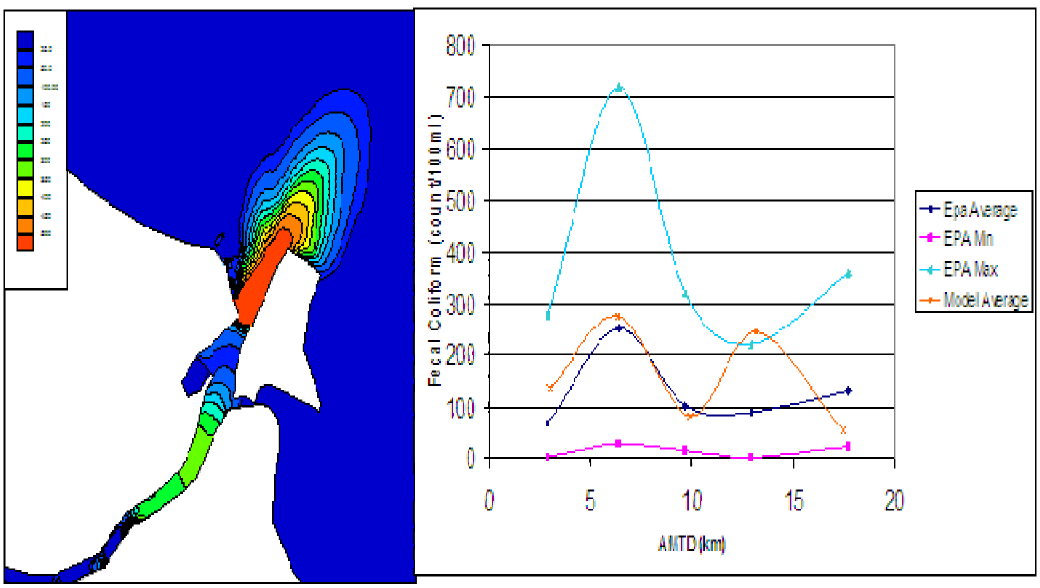


**Fig. 14. Predicted distribution of fecal coliforms (count/100 ml) for the lower Brisbane River and comparison with QEPA data**

## 3D SHYFEM Model of Cohesive Sediment Transport during 1996 Flood Flows to Moreton Bay

Cohesive sediment transport in Moreton Bay was modeled using the 3D version of SHYFEM for the flood flow period that occurred during May-June 1996. SHYFEM utilizes the Sedtrans 05 algorithms to model cohesive (e.g. mud) and non-cohesive sediments (e.g. sand) (see Ferrarin et al. 2006; 2009 for details). The cohesive sediment algorithms are designed to model a full cycle of erosion/deposition and the consolidation process. Particular care is taken to conserve sediment mass during the erosion, deposition and consolidation processes. SHYFEM allows for the modeling of a range of sediment class sizes. Each suspended particle is assumed to have a characteristic settling velocity $W_s$, which is determined during the erosion process when the particle is put into suspension; this it retains until the particle is deposited. This $W_s$ is modified temporarily to take account of flocculation. The bed shear stress resulting from both water currents and wind driven wave effects is corrected for two phenomena that might take place in the presence of cohesive sediments namely, drag reduction due to high suspended sediment concentrations and the solid-transmitted-stress by free moving vegetation (e.g. *Ulva* spp. *Lyngbya* spp.). Drag-reduction is included to avoid the continuous ongoing erosion of a poorly consolidated bed that would otherwise produce unrealistically high suspended sediment concentrations.

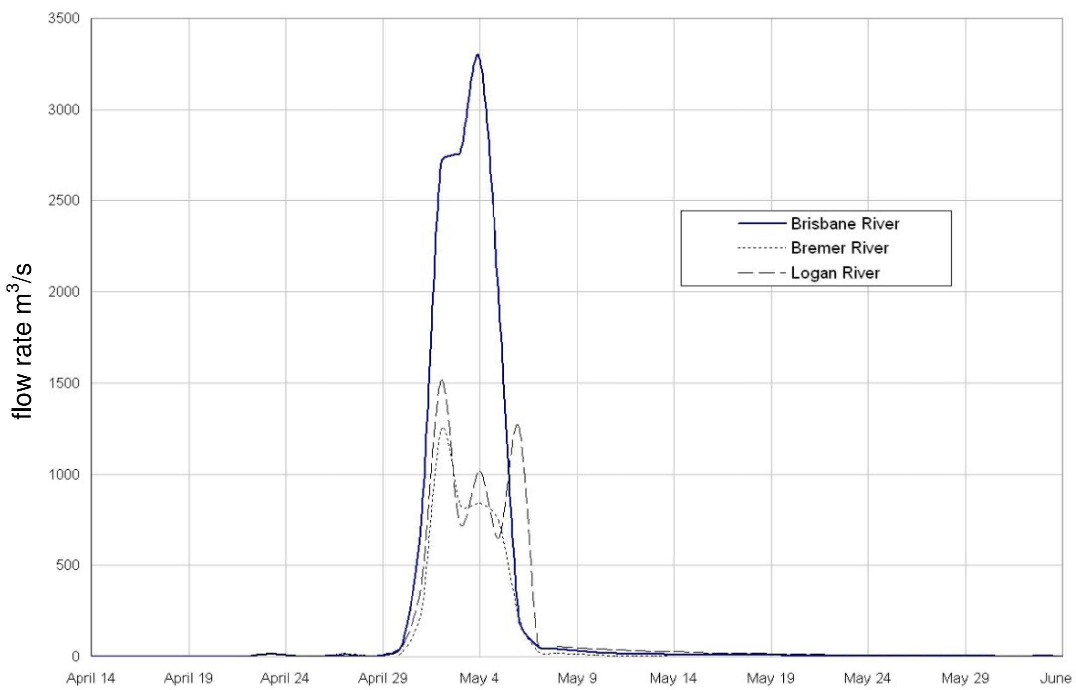


**Fig. 15. Hydrographs of 3 major freshwater inflows over simulation period (April-June 1996**

***May 1996 flood simulation***

Freshwater inputs and sediment loads to the various sub-catchments over the flood event period (April - June 1996 see Fig. 15) were determined using the AQUALM model (Anon, 1997a; McEwan, 1998). Total sediment loading over the period was 1.1 x $10^6$ tonnes with the upper Brisbane River catchments contributing 65% of the sediment load. The model set-up differed somewhat from that used in the RMA simulations in that the ocean boundary was extended some 50-100 km offshore (see Fig.16). This was done to simplify the specification of realistic boundary conditions to the system and in particular to avoid the necessity of setting time-varying stratified boundary conditions at the Bay-ocean boundaries.

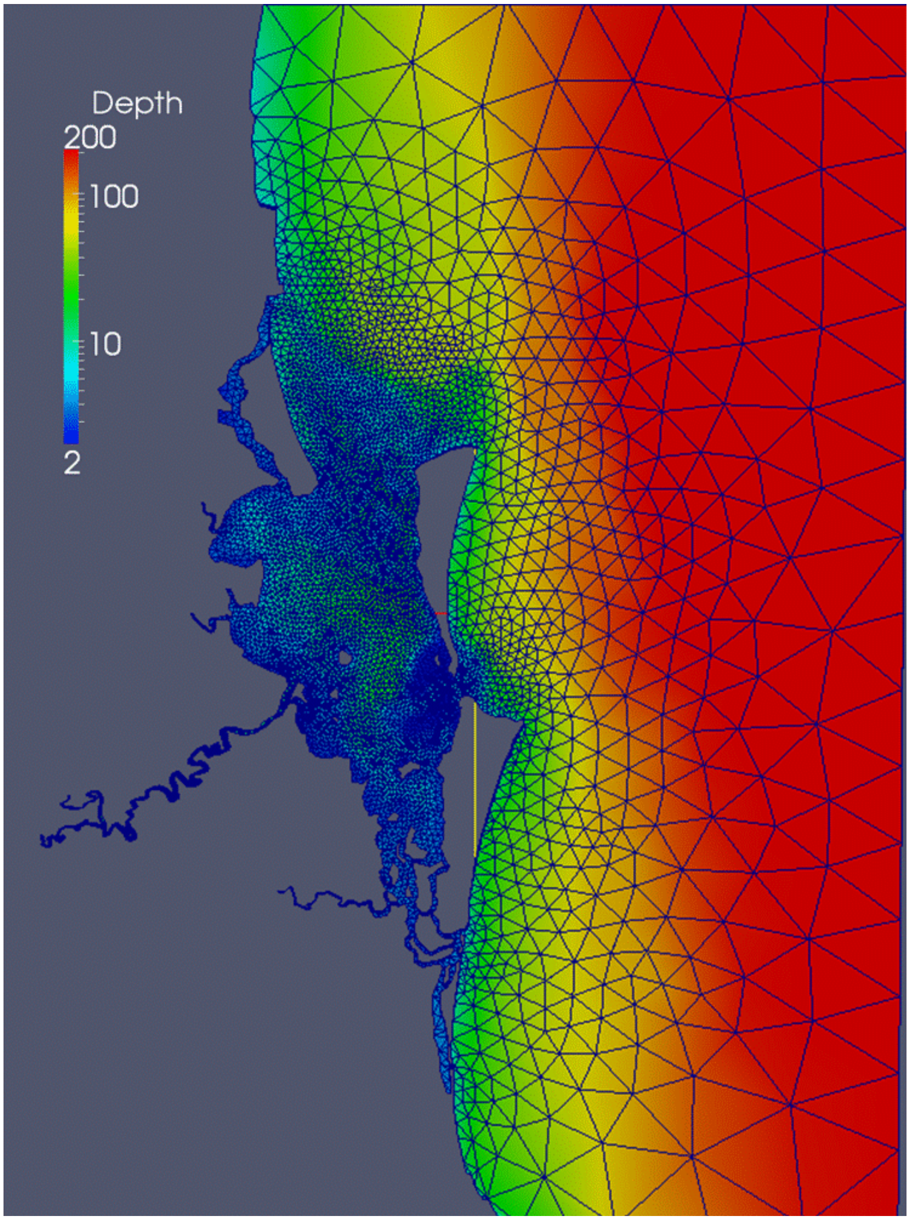


**Fig 16. Large scale high resolution finite element mesh used for SHYFEM 3D model.**

***Simulation results***

The results (see Figs 17-20) suggest that the influence of the turbid freshwater flows during the 1996 flood would have been widespread. Salinity stratification of waters in the lower reaches of the rivers (e.g. see Figs 17 - 19) would have been severe during the high flood-flow periods. Such conditions could lead to low dissolved oxygen in the lower saline layers which could lead to fish kills. Further work is underway to investigate such effects using the full 3D water quality model.

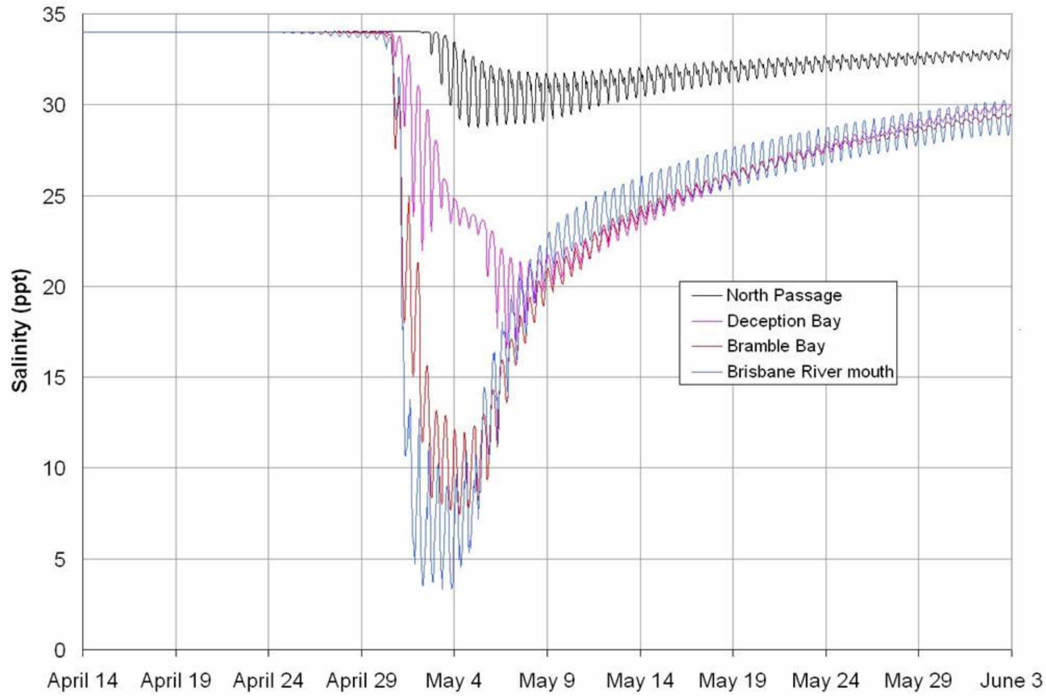


**Fig. 17. Predicted surface salinity at selected locations over simulation period (April 14-June 3 1996)**

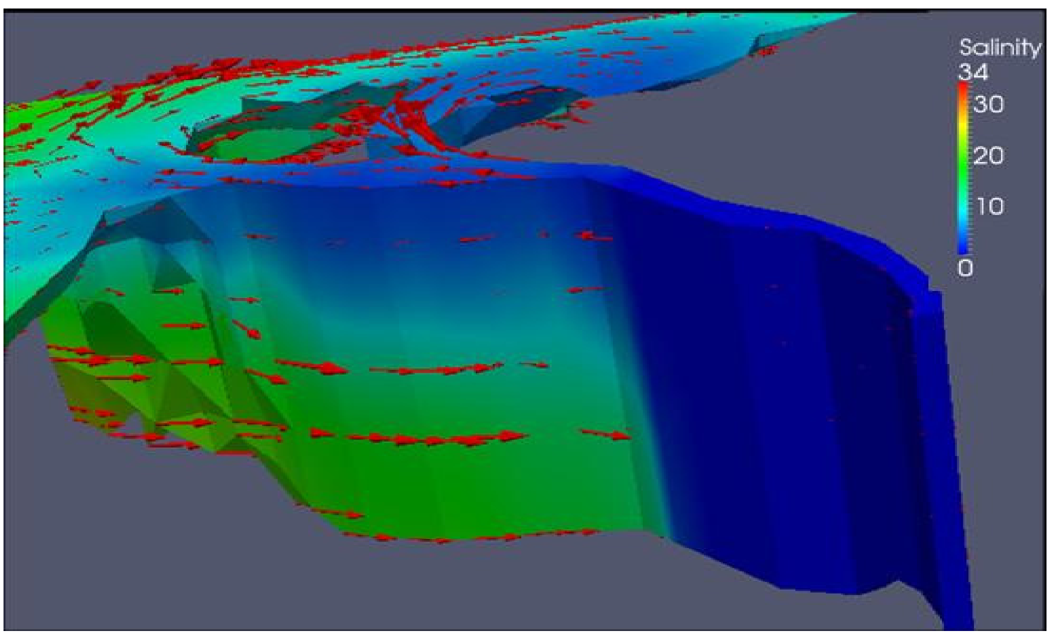


**Fig. 18. Predicted salinity distribution and velocity vectors at mouth of Brisbane River during 1996 flood flows**

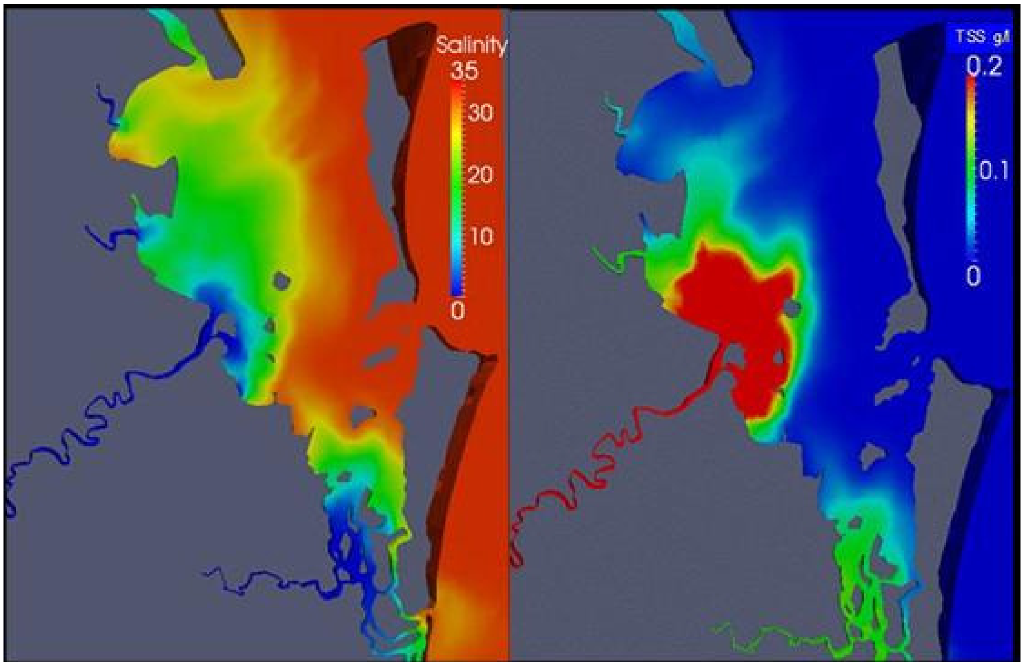


**Fig. 19. Predicted salinity (ppt) and total suspended solid (TSS g/l) distributions during 1996 flood flow.**

A comparison of the results from the simulation of cohesive sediment sedimentation with measured mud distribution results (Anon, 1997b; see Fig. 20) suggests that that the flood waters contribute significant amounts of muddy sediment to the Bay and much of that sediment is retained in the Bay.

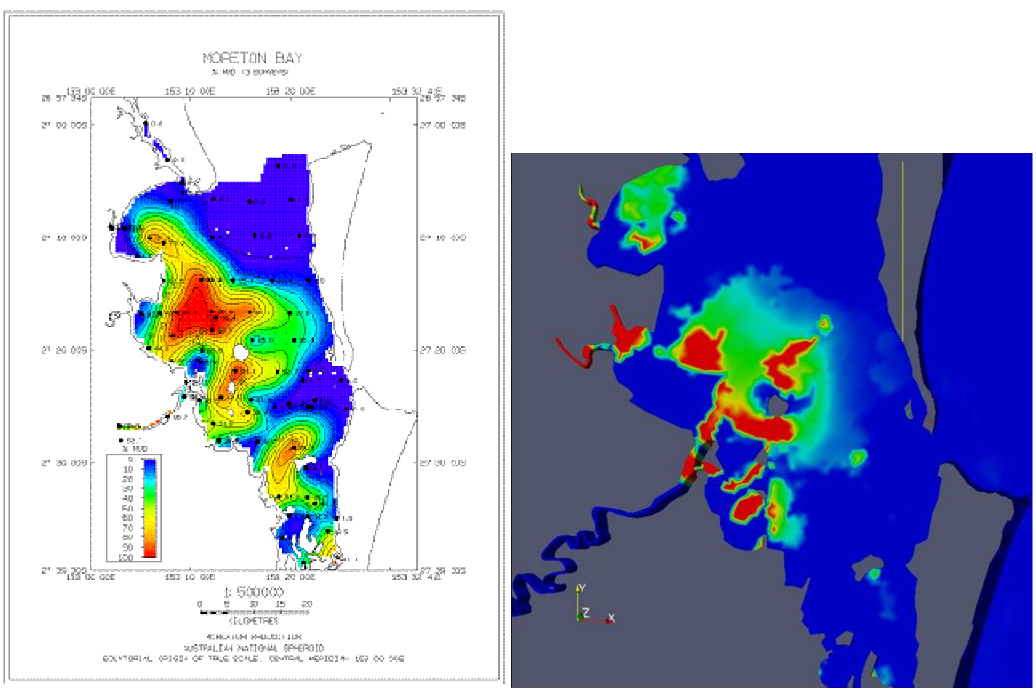


**Fig. 20. Comparison of measured and predicted regions of mud-deposition in Moreton Bay**

## Conclusions

The WWTP discharges have a significant impact on the dissolved oxygen and nutrient content of waters in the Brisbane-Bremer estuary and the nutrients discharged to Moreton Bay promote high levels of phytoplankton growth. The WWTP discharges are the principal source of phosphorus (FRP) during "dry-weather". FRP behaves as a passive tracer and hence can be used to track the influence of the WWTP discharges and to calibrate the transport model. The turbidity in the Brisbane River during "dry weather" results from the combined effects of tidal resuspension/flocculation of the sediments and the tidal-flow asymmetry induced by the baseline freshwater flow. The tidal pumping of resuspended sediments from the Bay is sufficient to provide the observed high turbidity in the Brisbane River estuary. Floodwaters impact significantly on the estuarine and Bay waters and provide a significant source of muddy sediments to the Bay.

## References


Anon. (1997a). TASK PL2: Catchment run-off loads. Report prepared for The Brisbane River and Moreton Bay Wastewater Management Study by WBM Oceanics, Brisbane.

Anon. (1997b). Design and Implementation of Baseline Monitoring. Report prepared for The Brisbane River and Moreton Bay Wastewater Management Study.

Ambrose, R.A., Wool, T.A., Connolly, J.P. & Schanz, R.W. (1993), WASP5, a hydrodynamic and water quality model : model theory, user's manual and programmer's guide, Envir. Res. Lab., Athens, Georgia. EPA/600/3-87/039.

Bell P. R. F. Bell, McEwan, J. and Coombs, S (2003). Finite Element Water Quality Model of the Moreton Bay System. Proceedings of the Sixth International Conference on the Mediterranean Coast Environment, MEDCOAST 03, Turkey, vol 1-3. pp. 1223-1234.

Bell, P., Coombs, S., and McEwan, J. (2002), 3 Dimensional Modelling of Turbidity in Brisbane River Estuary using RMA10 and RMA11, Final Report to CRC-CZEWM for RT/SM Tasks, Univ. of Queensland.

Brown, L.C. & Barnwell, T.O. (1987). The enhanced stream water quality models QUAL2E and QUAL2E-UNCAS. USEPA.

Ferrarin, C., E. Molinaroli, G. Umgiesser, (2006) A sediment transport model for the lagoon of Venice Universita Ca Foscari di Venezia Anno Accademico 2005-2006

Ferrarin C., Cucco A., Umgiesser G., Bellafiore D., Amos C (2009). Modelling fluxes of water and sediment between Venice Lagoon and the sea. Continental Shelf Research, doi:10.1016/j.csr.2009.08.014

King I. P. (2005) RMA-11 -- A three dimensional finite element model for water quality in estuaries and streams version 4.3a Resource Modelling Associates Sydney, Australia.

King, I. (1997), "A three dimensional finite element model for water quality in estuaries and streams", Dept. of Civ. and Envir. Eng. University of California.

McEwan J., Gabric AJ and Bell PRF (1998). Water quality and phytoplankton dynamics in Moreton Bay (SE Queensland) II. Mathematical Modelling. Mar.Freshwater Res. 49, 227-39

McEwan, J. (1996), "A coupled hydrodynamic, transport and kinetic model of eutrophication processes in Moreton Bay, Queensland. PhD Thesis, Uni. of Queensland.

McEwan, J. (1998) Cohesive sediment dynamics in RWQM2. Report prepared for the Brisbane River and Moreton Bay Wastewater Management Study, February 1998.

Umgiesser, G., D. Melaku Canu, C. Solidoro, and R. Ambrose. (2003). A finite element ecological model: a first application to the Venice Lagoon. EMS, 18(2):131–145.
Umgiesser, Georg, Donata Melaku Canub, Andrea Cucco, Cosimo Solidoro (2004). A finite element model for the Venice Lagoon. Development, set up, calibration and validation Journal of Marine Systems 51 123– 145

## Appendix A

The water quality models can simulate up to 30 system variables. The systems can be simulated in both the water column and in the benthos/sediments.

**Table A1-Water Quality Variables**

| Variablel No. | Description |
|---|---|
| 1 | arbitrary Non-Conservative (1) |
| 2 | BOD1 |
| 3 | BOD2 |
| 4 | BOD3 |
| 5 | BOD4 |
| 6 | dissolved oxygen |
| 7 | organic nitrogen 1 |
| 8 | organic nitrogen 2 |
| 9 | organic nitrogen 3 |
| 10 | organic nitrogen 4 |
| 11 | ammonia nitrogen |
| 12 | oxidised nitrogen |
| 13 | organic phosphorous 1 |
| 14 | organic phosphorous 2 |
| 15 | organic phosphorous 3 |
| 16 | organic phosphorous 4 |
| 17 | inorganic phosphate |
| 18 | Si |
| 19 | Fe |
| 20-22 | phytoplankton carbon (3 types) |
| 23 | temperature |
| 24 | cohesive suspended sediment |
| 25 | sand |
| 26 | salinity |
| 27 | coliforms |
| 28 | arbitrary non-conservative (2) |
| 29 | arbitrary non-conservative (3) |
| 30 | arbitrary non-conservative (4) |

In general the same governing equations are used in both the water column and benthos. All rates have a Arrhenius-type temperature-dependence. For simplicity this is omitted from the equations.

## Algal growth

Phytoplankton is modelled in units of carbon with a fixed C:N:P stoichiometry (Fig. A1). The general equation for growth is :

$$\frac{dS_4}{dt} = (\mu - d - r - g)S_4$$

where,

| | | |
|---|---|---|
| $S_4$ | = | phytoplankton carbon biomass ($mgL^{-1}$) |
| $\mu$ | = | specific growth rate ($day^{-1}$) |
| $d$ | = | non-predatory death rate ($day^{-1}$) |
| $r$ | = | respiration rate ($day^{-1}$) |
| $g$ | = | herbivorous zooplankton grazing rate ($day^{-1}$) |

The instantaneous growth rate $\mu$ is obtained from :

$$\mu = \mu_m \, g_1 g_2 g_3$$

where,

$\mu_m$ = average saturated growth rate at 20ºC ($day^{-1}$)

$g_1$, $g_2$, $g_3$ =growth-rate modifying coefficients for light, temperature and nutrient availability respectively.

Monod relationships are used to calculate the growth limitation factors for N, P, Fe and Si availability :

## Sediment – water column particulate exchanges

Particulate constituents can settle to the benthos at a fixed settling rate. Resuspension of benthic particulate material (particulate C, N, P and benthic phytoplankton) is driven by time- and spatially-variable bottom shear stress. The algorithms for determining bottom shear stress as a function of wind waves and tidal currents are described elsewhere (McEwan, 1998).

## Coliforms

Coliform transport is modelled using three loss parameters:

1. settling
2. decay in darkness
3. light sensitive decay.

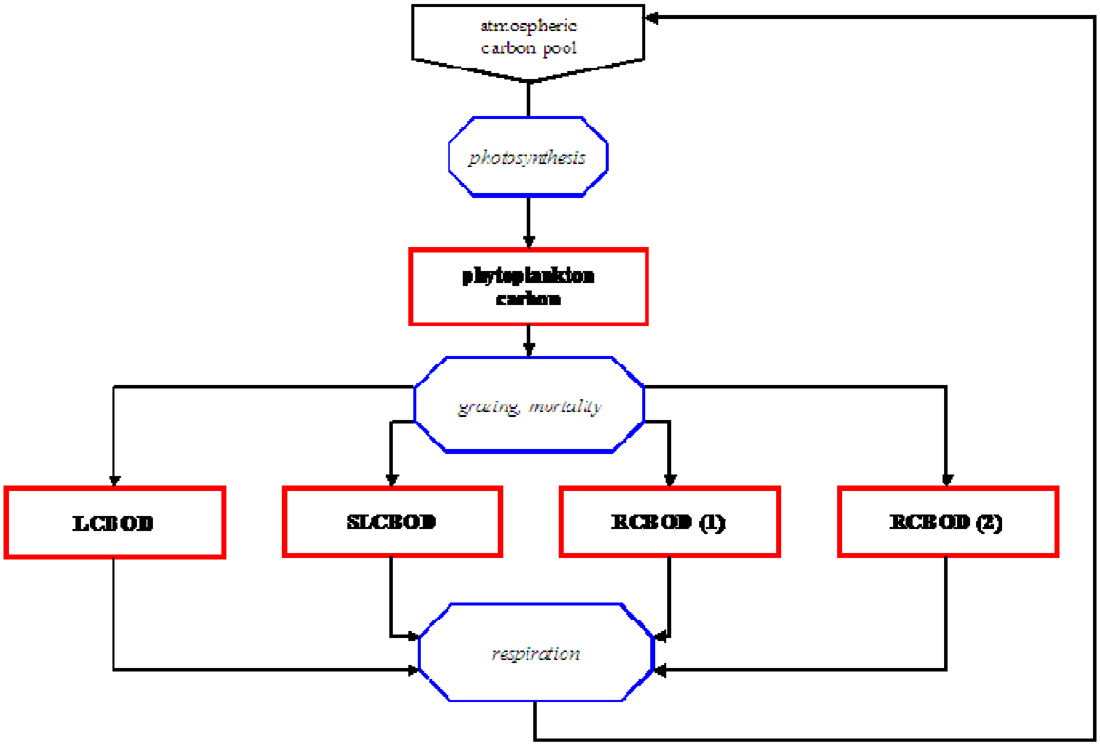


**Fig. A1. Carbon cycling.**

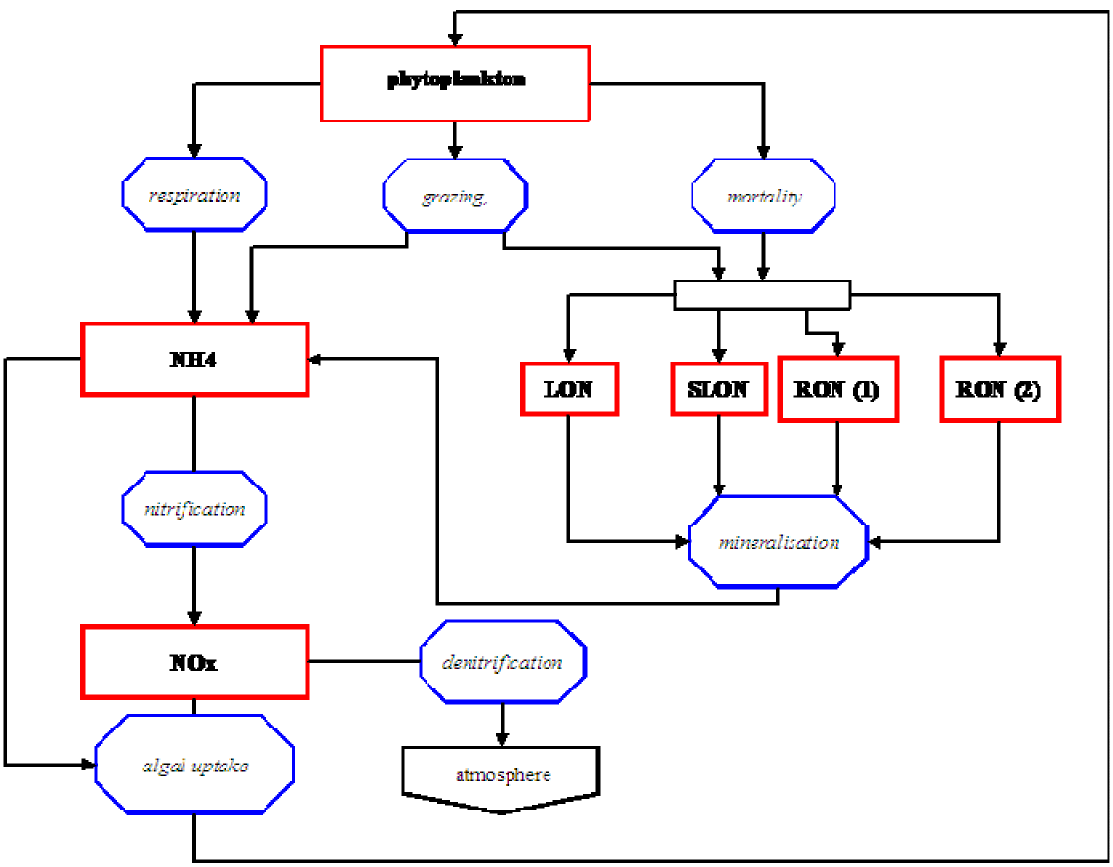


**Fig. A2. N cycling.**

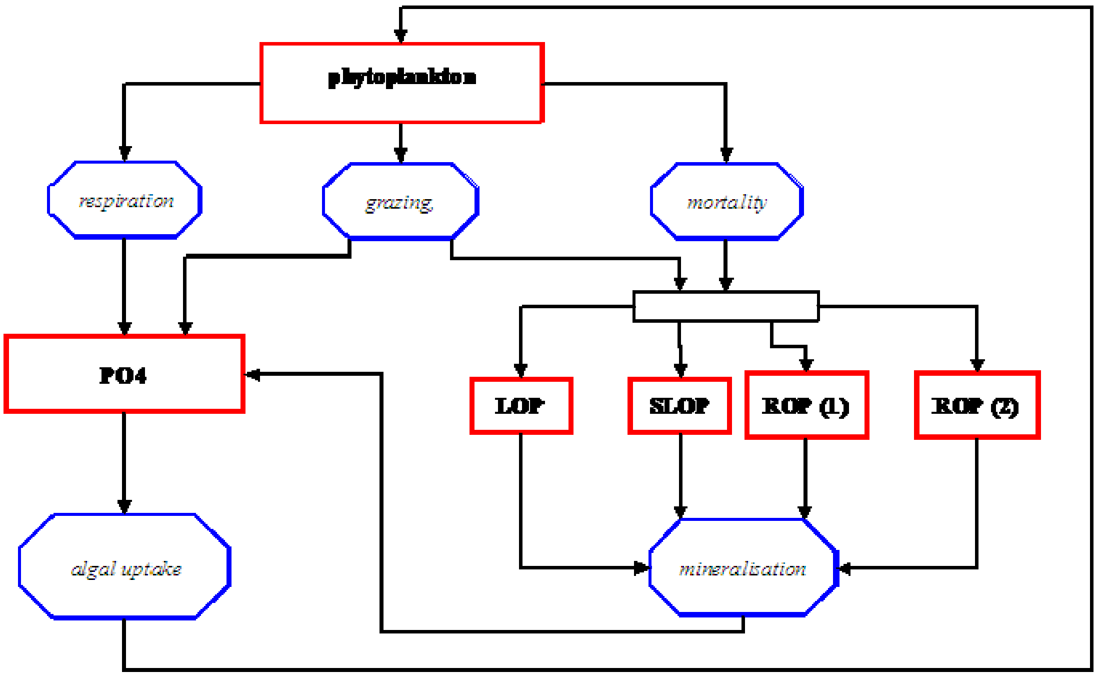


**Fig. A3. P cycling**

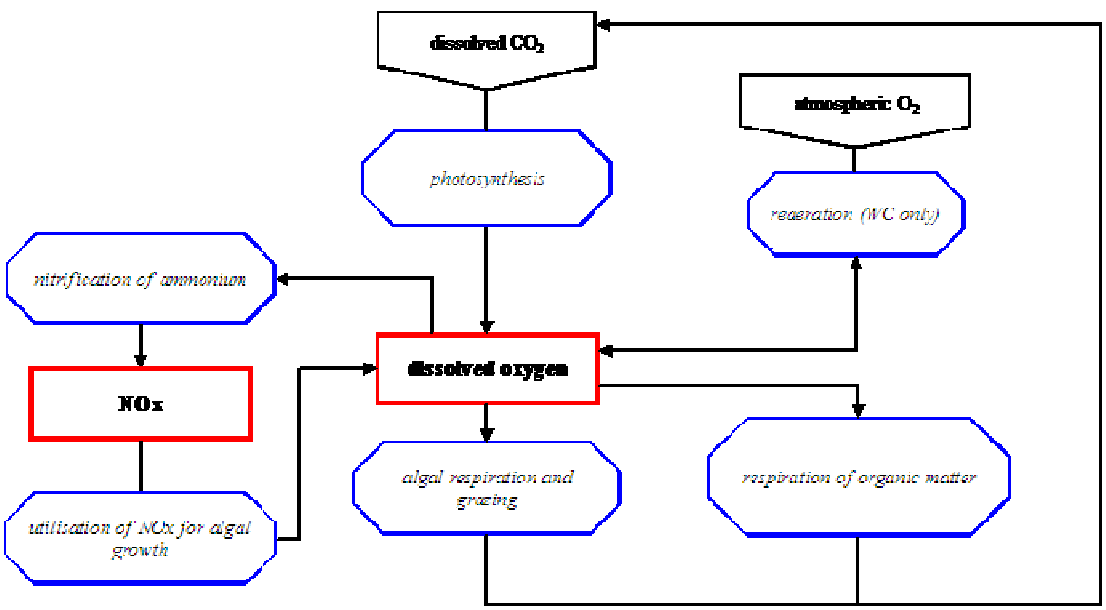


**Fig. A4. DO cycling**